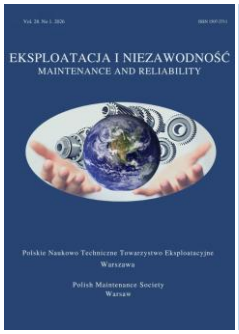

Eksploatacja i Niezawodnosc – Maintenance and Reliability

Volume 28 (2026), Issue 1

journal homepage: http://www.ein.org.pl

Article citation info:
Hu C, Xianming S, Cui X, Wang Y, Reliability Estimation of Retraction Mechanism Kinematic Accuracy under Small Sample, Eksploatacja i Niezawodnosc – Maintenance and Reliability 2026: http://doi.org/10.17531/ein/216106

Reliability Estimation of Retraction Mechanism Kinematic Accuracy under Small Sample

Indexed by: Web of Science Group

Cenyu Hu[a], Shi Xianming[a,*], Xiaolu Cui[b], Yalong Wang[a]

[a] Army Engineering University of the PLA Shijiazhuang Campus, China
[b] Army Engineering University, China

Highlights

- Shows model outperforms traditional ones, reducing parameter uncertainty effectively.
- Solves high-dimensional posteriors via MCMC Gibbs sampling, verifying convergence.
- Bayesian inference, using normal and inverse gamma as conjugate priors.
- Uses working cycles as life index to construct residual strength.
- Proposes a Bayesian framework for time-varying reliability estimation.

Abstract

New equipment testing, constrained by environment and cost, yields limited reliability data, hindering accurate estimation. This paper proposes a Bayesian framework for time-varying reliability estimation and remaining life prediction of small-sample equipment. Using working cycles as the life index, it constructs residual strength of fatigue damage accumulation and derives the time-varying reliability function. To address poor parameter estimation with small samples, Bayesian inference fuses prior information with field test data. Normal and inverse gamma distributions are chosen as conjugate priors to derive posterior distributions of initial strength and working load parameters, plus maximum posterior estimates. High-dimensional posteriors are solved via Gibbs sampling in MCMC, with convergence verified. Empirical analysis shows the model outperforms traditional ones. Integrating prior and experimental data makes the posterior distribution more centralized than the prior, reducing parameter uncertainty.

Keywords
bayesian inference, time-varying reliability, remaining life prediction, small sample data, MCMC

1. Introduction

The reliability of new equipment is a core indicator of operational effectiveness and safety. However, its development is hampered by inherent design flaws, which rigorous reliability testing aims to expose. Such testing faces two primary challenges in the R&D phase: (1) the prohibitive cost and long manufacturing cycles for components like high-voltage relays 1 and permanent magnet brakes 2 result in severely scarce test data; and (2) traditional large sample based assessment methods (e.g., maximum likelihood estimation) suffer from high variance and misjudgment under such data-scarce conditions 4. Although a large number of simulation tests have provided abundant prior knowledge about material properties and load responses, the lack of an effective integration mechanism prevents these pieces of information from compensating for the absence of physical test data. Consequently, achieving accurate reliability estimation under small-sample conditions by integrating simulation information with limited field data has become an urgent problem in reliability engineering 5.

Engineering practice shows equipment life follows diverse distributions 6,with the normal distribution being prevalent for cyclically loaded mechanical equipment 7. Owing to its theoretical tractability, computational simplicity, and broad

(*) Corresponding author.
E-mail addresses: C. Hu (ORCID: 0009-0005-4765-8525) 1339816023@qq.com, S. Xianming (ORCID: 0000-0003-3576-8952) 17700093117@163.com, X. Cui (ORCID: 0009-0005-3772-8382) 13940806458@163.com, Y. Wang (ORCID: 0009-0007-3767-0154) jsydb@qq.com,

applicability (Weibull or lognormal distributions can often be transformed to approximate it), it becomes a convenient and reasonable choice for reliability modeling. Therefore, this paper focuses on equipment whose life is primarily characterized by a normal distribution.

Existing research on equipment reliability assessment can be systematically categorized into three types based on technical principles, each with distinct research significance and core findings:

1) **Intelligent Algorithm-based Methods**

This type of method leverages nonlinear fitting and adaptive learning capabilities to handle complex reliability relationships, which is of great significance for solving reliability assessment problems under multi-source monitoring data scenarios.

Literature 8 proposed an improved SSD network combined with infrared image processing technology to construct an intelligent detection system for electrical equipment with a mAP value of 92.58% after 1200 iterations, providing an accurate solution for equipment abnormal state identification; Literature 9 used YOLOv3 algorithm fused with image segmentation algorithm technology to achieve bridge damage of accurately locating defects, which verifies the practical value of neural networks in the reliability of large-scale engineering equipment; Literature 10 designed a real-time monitoring system for digital grid equipment, which combines the advantages of traditional statistical methods, machine learning, and deep learning, and realizes high reliability of fault prediction; Literature 11 for the problem of anomaly detection of oil reservoir prospecting data and intelligent diagnosis problem, proposed to combine learners such as decision tree and support vector machine (SVM), and use the Boosting integrated learning strategy and adaptive thresholding mechanism.

However, most of these intelligent algorithm studies focus on equipment reliability assessment under large-sample conditions 12. Due to the high experimental cost and long cycle of new equipment testing, small-sample scenarios are common, and intelligent algorithms often suffer from overfitting and poor generalization ability in such scenarios. 13.

2) **Bayesian Statistical Methods**

As the core method for small-sample reliability assessment, Bayesian statistical inference has a significant advantage in information fusion. It can integrate prior information (such as historical data, expert experience, and simulation results) with limited experimental data, which is of great significance for improving the accuracy of parameter estimation under small-sample conditions.

Literature 14 used Bayesian method to fuse historical data of similar equipment to achieve the reliability assessment of a continuous k-out-of-n : F system; Literature 15 developed a Weibull regression model within the Bayesian probabilistic framework with covariate selection, and estimated model parameters with associated uncertainties based on a small amount of data and expert judgment to be used for reliability estimation of industrial equipment. Literature 16, on the other hand, performed Bayesian inference of destruction effectiveness based on Bayesian multinomial distribution. Literature 17 directly explored Bayesian modeling of test reliability. Literature 18 combined digital twin techniques with the Bayesian framework to achieve 99.248% fault diagnosis accuracy through the AL-DNN algorithm to construct a safe error prevention mechanism in zero-defect manufacturing;

Although most Bayesian studies can fuse historical data and expert experience, they often ignore the role of simulated experimental information in correcting prior distributions 1920. Literature 21 proposed a reliability assessment method for aerospace valves and realized multi-source information fusion, but it did not integrate finite element simulation data of valves. In fact, simulation data can provide information about the fatigue damage law of equipment under extreme conditions, which is crucial for improving the rationality of prior distributions.

The residual strength degradation of equipment under cyclic loading is a highly nonlinear and stochastic process, which leads to high-dimensional posterior distributions of model parameter. Traditional analytical methods cannot directly solve these high-dimensional distributions, and numerical methods such as MCMC are usually required 22. However, existing studies either lack detailed verification of the convergence of MCMC sampling or have complex implementation processes, which affects the accuracy and efficiency of parameter estimation.

3) **Classical Statistical Correction Methods**

The Bootstrap self-help method expands the sample size through data resampling and introduces virtual samples to assess the stability and uncertainty of statistical quantities when

the original data is insufficient 23. This method is easy to implement and does not require prior distribution assumptions, making it suitable for reliability assessment of equipment with unknown prior information. However, its accuracy depends heavily on the representativeness of the original small sample—if the original sample has sampling bias, the expanded sample will inherit this bias 24.

Furthermore, research specifically focusing on the dynamic evolution of equipment reliability over time—known as time-varying reliability—has formed an important branch of study. Accurately assessing this temporal evolution is crucial for evaluating equipment condition throughout its entire life cycle 25. The core of these methods lies in establishing performance degradation models (stochastic models based on the Wiener or Gamma processes 2627) to describe the evolution of key parameters, such as equipment strength and wear, with working cycles or time, thereby enabling residual life prediction.

However, when applied to the small-sample scenarios central to this work, existing time-varying reliability methods face significant challenges:

First, parameter estimation for most degradation models relies heavily on abundant historical failure or degradation data to ensure statistical significance, a condition often unmet during the development of new equipment28.

More critically, existing research shows a notable deficiency in integrating multi-source information to compensate for data scarcity. Although numerical simulations can provide valuable prior knowledge about the dynamic degradation process of equipment , effective mechanisms are currently lacking to integrate this "time-varying prior information" with sparse field-test data. This often leads to degradation models built from small samples having substantial uncertainties, making it difficult to accurately capture the true temporal evolution of reliability 29.

In summary, while the methods discussed above have advanced the field in their respective domains, they exhibit inherent limitations when addressing the compounded challenge of time-varying reliability assessment under small-sample conditions. These limitations include inadequacy with small samples, underutilization of simulation information, and insufficient modeling of dynamic degradation processes.

To overcome these limitations, this paper proposes a time-varying reliability and residual life prediction method that integrates multi-source information for cyclically loaded equipment. First, we develop a residual strength degradation model that accounts for cumulative fatigue damage, quantifying the load-strength coupling relationship with working cycles as the life index. This model overcomes the limitations of traditional approaches in capturing nonlinear stochastic degradation. Second, we fuse simulated and field-test data to establish conjugate prior distributions for initial strength and load parameters, deriving maximum a posteriori estimates. To address the high-dimensional posterior, we employ a Gibbs sampling algorithm for MCMC inference, with convergence diagnostics ensuring validity. Finally, a case study demonstrates the superior accuracy of our model under small-sample conditions compared to traditional empirical models, highlighting the advantage of our approach.

2. The time-varying reliability model based on the number of working cycles

2.1. Model Assumptions and Description

New equipment in the actual operation process often faces complex dynamic load environments. This load has strong impact and cyclic loading characteristics, which will lead to fatigue damage of key component materials. To construct an engineering-applicable life prediction model, the following idealized assumptions are proposed with rational justifications:

I. Based on the fatigue test data from reference 7, when the equipment is shut down, its components are in a static state; the contribution of environmental factors (such as temperature and humidity) to fatigue damage is less than 5%. Therefore, when the equipment is shut down, the influence of environmental factors is ignored, and only the cumulative effect of dynamic loads during operation is considered. It is assumed that the amplitudes of each run's load are independent of each other and follow the same probability distribution.

II. Based on literature 13 , the p-value of the K-S test for the initial strength is 0.87, which is greater than 0.05. This indicates that the normal distribution is applicable. Therefore, the initial strength of the key components of the equipment obeys a normal distribution as $R_0 \sim N(\mu_R, \sigma_R^2)$,where $\mu_R$is the average load carrying capacity of the material, and σ_R is to reflect the dispersion of the components in the same batch.

III. Based on the Literature 16, the launching load Sobeys the normal distribution $S\sim N(\mu_S,\sigma_S^2)$ where μ_S is the mean value of the load and σ_S reflects the range of load fluctuation. When the coefficient of variation $CV=\sigma_S/\mu_S<0.1$, the load can be regarded as "quasi-static", which is convenient for simplified engineering calculations.

IV. Based on the Literature 21, the residual strength $R(n)$ is related only to the magnitude of the load and the number of work cycles n, ignoring secondary factors such as geometric deformation.

2.2. Residual strength degradation modeling and reliability function derivation

2.2.1. Residual strength degradation model

The residual strength degradation model after the device has undergone n duty cycles is:

$$R(n)=R_0-\sum_{i=1}^{n}k\left(\frac{S_i}{S_e}\right)^m \tag{1}$$

where R_0 is the initial strength of the device, S_i is the ith working load; k and m are the material fatigue parameters, which are determined by accelerated life tests.; S_e is the reference load (taken as the average value of the load under the standard test conditions of the device). S_e standardizes the working load $S_i$to eliminate the dimensional differences among different load magnitudes, thereby making the fatigue damage accumulation term $(S_i/S_e)^m$ dimensionless. This ensures that the model is comparable under different equipment or working conditions.

Since the initial strength R_0 and the working load S_i are both random variables, the residual strength $R(n)$ is a composite random variable. When $R(n)<S(n)$, failure of the device occurs, and the failure critical state is defined as $R(n)=S(n)$.

This criterion is consistent with the stress-strength interference theory 4, When $R(n)<S(n)$: The residual strength of the equipment exceeds the working load it bears, and the component can withstand cyclic loading without fatigue failure; When$R(n)<S(n)$:The load exceeds the component's residual strength, leading to rapid propagation of fatigue cracks or plastic deformation, which directly causes equipment failure.

2.2.2. Reliability function derivation

The event A_n is "the equipment did not fail after the nth working cycle", then the reliability $R(n)$ is A_n.According to the stress-strength interference theory, the reliability of the equipment for the first working cycle is the probability that the initial strength R_0 is greater than the 1st load S_1:

$$\begin{aligned}R(1)&=P(R_0>S_1)=\int_{-\infty}^{+\infty}f_s(s)\left[\int_{s}^{+\infty}f_s(s)dr\right]ds\\&=P(R_0-S_1>0)\end{aligned} \tag{2}$$

where $f_{R_0}(r)=\frac{1}{\sqrt{2\pi}\sigma_R}e^{-\frac{(r-\mu_R)^2}{2\sigma_R^2}}$ and $f_S(r)=\frac{1}{\sqrt{2\pi}\sigma_S}e^{-\frac{(s-\mu_S)^2}{2\sigma_S^2}}$ are the probability density functions of the initial strength and working load, respectively.

According to the assumption condition (iii), considering the independence of n working cycles of the equipment, the reliability after the nth cycle is the joint probability of the nth non-failure under the previous $n-1$ non-failure conditions:

$$\begin{aligned}R(n)&=P(A_1\cap A_2\cap\cdots\cap A_n)\\&=P(A_n\mid A_{n-1}\cap\cdots\cap A_1)\cdot R(n-1)\end{aligned} \tag{3}$$

The conditional probability expansion can be obtained:

$$R(n)=\prod_{i=1}^{n}(R(i)>S(i)|R(i-1)>S(i-1)) \tag{4}$$

The residual strength degradation model Eq. (1) is substituted into Eq. (4):

$$R(n)=\int_0^{\infty}\prod_{i=1}^{n}F_s\left(R_0-k\sum_{j=1}^{i}\left(\frac{S_j}{S_e}\right)^m\right)f_{R_0}(r_0)dr_0 \tag{5}$$

Considering the randomness of the initial intensity R_0,the expectation of Eq. (5) over the distribution of R_0 is obtained:

$$R(n)=\int_0^{\infty}\left[1-F_s\left(r_0-k\sum_{i=1}^{n}\left(\frac{S_i}{S_e}\right)^m\right)\right]f_{R_0}(r_0)dr_0 \tag{6}$$

where $F_s(s)$ is the cumulative distribution function of the working load. Since $\sum_{i=1}^{n}(S_i/S_e)^m$ is a nonlinear combination of multiple random variables, it is difficult to solve it directly, and it needs to be simplified and calculated by probability statistics. (see section 2.2.3)

2.2.3. Quantification of stochastic characteristics in time-varying reliability

The initial strength and working load of the new equipment are random variables that need to be described by probabilistic statistical methods. Assuming the initial strength $R_0\sim N(\mu_R,\sigma_R^2)$, the work load $S\sim N(\mu_S,\sigma_S^2)$, after substituting into the probability density function of the normal distribution, Eq. (6) can be expanded as:

$$R(n)=\frac{1}{\sqrt{2\pi}\sigma_R}\int_{-\infty}^{+\infty}\left[1-\Phi\left(\frac{r-k\sum_{j=1}^{i}\left(\frac{S_j}{S_e}\right)^m}{\sigma_S}\right)\right]e^{-\frac{(r-\mu^R)^2}{2{\sigma_R}^2}}dr \tag{7}$$

where $\Phi(\cdot)$ is the cumulative distribution function of the

standard normal distribution used to quantify the probability that the load $S$is less than the critical value.

The difference between the residual strength of equipment and load, $Z(n) = R(n) - S(n)$,follows a normal distribution, denoted:

$$Z(n) \sim N(\mu_R - n \cdot k(\frac{\mu_S}{S_e})^m - \mu_S, \sigma_R^2 + \sigma_S^2) \tag{8}$$

The mean and variance are respectively:

$$\begin{aligned} \mu_z &= E[R_0] - n \cdot k(\mu_s / S_e)^m - E[S_n] \\ &= \mu_R - n \cdot k(\mu_s / S_e)^m - \mu_s \end{aligned} \tag{9}$$

$$\sigma_z^2 = Var(R_0) + Var(S_n) = \sigma_R^2 + \sigma_S^2 \tag{10}$$

At this point the reliability is the probability that $Z(n) > 0$. When the load coefficient of variation $CV = \sigma_S/\mu_S < 0.1$, the amount of strength degradation per duty cycle can be approximated as its expected value:

$$E[k(\frac{S}{S_e})^m] \approx k(\frac{\mu_S}{S_e})^m \tag{11}$$

Therefore, the total degradation after n cycles is $n \cdot (k/S_e)^m$, which can be used as a load-averaged μ_S instead of the random variable S_i , in which point Eq. (7) simplifies to:

$$R(n) = \Phi(\frac{\mu_R - k \cdot n(\frac{\mu_S}{S_e})^m - \mu_S}{\sqrt{\sigma_R^2 + \sigma_S^2}}) \tag{12}$$

The model reveals the degradation law of equipment reliability with the number of duty cycles$n$. For new equipment testing, the full life cycle data are often limited (only 10-20 sets of valid samples can be obtained), which leads to insufficient parameter estimation accuracy of traditional methods.

In view of this, the Bayesian estimation method can be introduced to derive the posterior distribution of the parameters and solve for the maximum a posteriori estimates by fusing the prior information with the small-sample test data.

3. Posterior estimation based on Bayesian inference

To address the problem of limited sample size in the testing of new equipment, it is assumed that both the initial strength of the equipment and the working loads obey the normal distribution, i.e., $R_0 \sim N(\mu_R, \sigma_R^2)$, $S \sim N(\mu_S, \sigma_S^2)$,where μ_R , μ_S are the mean values and σ_R^2 , σ_S^2 is the variance. The parameter estimation accuracy is improved by fusing the prior information with small sample data through Bayesian inference.

3.1. Bayesian framework for posterior parameter estimation

The parameter vector is $\theta = \{\mu_R, \sigma_R^2, \mu_S, \sigma_S^2\}$,the observation data is $D = \{R_0^1, R_0^2, \cdots, R_0^m; S_1, S_2, \cdots, S_n\}$, where R_0^i is the ith device's initial strength measured value, and S_j is the load data of the jth work cycle.

According to Bayes' theorem, the posterior distribution of the parameters is:

$$P(\theta|D) = \frac{P(D|\theta) \cdot P(\theta)}{P(D)} \propto P(D|\theta) \cdot P(D) \tag{13}$$

where $P(\theta)$ is the prior distribution, which integrates the historical data of similar devices and expert experience; $P(D|\theta)$ is the likelihood function, which describes the probability of occurrence of the parameter θ observed data; $P(\theta|D)$ is the posterior distribution, which means that The probability distribution of the parameter θ when the data D are known.

3.2. Derivation of posterior distribution parameters

The initial strength of the device R_0 (the derivation process of the working load S is the same), let R_0 obey the normal distribution $R_0 \sim N(\mu_R, \sigma_R^2)$, and the observation data is $D_R = \{R_0^1, R_0^2, \cdots, R_0^m\}$. According to Bayes' theorem, the posterior distribution of the parameter μ_R, σ_R^2 is:

$$P(\mu_R, \sigma_R^2|D_R) \propto P(D_R|\mu_R, \sigma_R^2) \cdot P(\mu_R) \cdot P(\sigma_R^2) \tag{14}$$

The likelihood function $p(D_R|\mu_R, \sigma_R^2)$ in the formula is

$$P(D_R|\mu_R, \sigma_R^2) = \prod_{i=1}^m \frac{1}{\sqrt{2\pi\sigma_R^2}} exp\left\{-\frac{(R_0^i - \mu_R)^2}{2\sigma_R^2}\right\} \tag{15}$$

To simplify the calculation, the prior distributions $P(\mu_R)$ and $P(\sigma_R^2)$ are chosen to take the normal and inverse gamma distributions as the conjugate prior distributions, respectively:

$$\mu_R \sim N(\mu_{R0}, \tau_{R0}^2) \tag{16}$$

$$\sigma_R^2 \sim IGa(\alpha_{R0}, \beta_{R0}) \tag{17}$$

where $IGa(\cdot)$ represents the inverse gamma distribution, and α_{R0}, β_{R0} are the hyperparameters of the prior distribution. Their values are obtained by fitting 30 sets of prior samples.

The inverse gamma distribution forms a conjugate pair with the normal likelihood function. The posterior distribution of the normal distribution is still the inverse gamma distribution. There is no need for complex integration to solve the posterior parameters, and the computational efficiency is higher than that of the Weibull distribution and the log-normal distribution.

By the conjugate prior property, the posterior distribution of

μ_R remains normal:

$$\mu_R|D_R \sim N\left(\frac{\tau_{R0}^{-2}\mu_{R0}+m\sigma_R^{-2}\overline{R_0}}{\tau_{R0}^{-2}+m\sigma_R^{-2}}, \frac{1}{\tau_{R0}^{-2}+m\sigma_R^{-2}}\right) \tag{18}$$

where $\overline{R_0} = \frac{1}{m}\sum_{i=1}^{m} R_0^i$ is the initial intensity sample mean.

The posterior distribution of the variance σ_R^2, combined with the inverse gamma prior and normal likelihood, σ_R^2 is still inversely gamma distributed:

$$\sigma_R^2|D_R \sim IGa\left(\alpha_{R0}+\frac{m}{2}, \beta_{R0}+\frac{1}{2}\sum_{i=1}^{m}\left(R_0^i-\mu_R\right)^2\right) \tag{19}$$

The work load S obeys a normal distribution $S \sim N(\mu_S, \sigma_S^2)$,the data are $D_S = \{S_1, S_2, \cdots, S_n\}$, and the prior distribution is:

$$\mu_S \sim N(\mu_{S0}, \tau_{S0}^2) \tag{20}$$

$$\sigma_R^2 \sim IGa(\alpha_{R0}, \beta_{R0}) \tag{21}$$

Similarly, the posterior distribution of the mean μ_R and variance σ_S^2 is:

$$\mu_S|D_S \sim N\left(\frac{\tau_{S0}^{-2}\mu_{S0}+n\sigma_S^{-2}\overline{S}}{\tau_{S0}^{-2}+n\sigma_S^{-2}}, \frac{1}{\tau_{S0}^{-2}+m\sigma_S^{-2}}\right) \tag{22}$$

$$\sigma_S^2|D_S \sim IGa\left(\alpha_{S0}+\frac{n}{2}, \beta_{S0}+\frac{1}{2}\sum_{j=1}^{n}\left(S_j-\mu_S\right)^2\right) \tag{23}$$

where $\overline{S} = \frac{1}{n}\sum_{j=1}^{m} S_j$ is the load sample mean.

3.3. Derivation of MAP parameter estimates

The prior distribution and likelihood function are substituted into Bayes' theorem, and the log posterior probability function is obtained by taking the logarithm:

$$ln\,P(\theta|D) = ln\,P(D|\theta) + ln\,P(\theta) \tag{24}$$

The μ_R, σ_R^2 of the initial intensity parameter of the new device, for example, has a log posterior probability of:

$$\begin{aligned} &ln\,P(\mu_R, \sigma_R^2|D_R) = \\ &-\frac{m}{2}ln\,\sigma_R^2 - \frac{1}{2\sigma_R^2}\sum_{i=1}^{m}(R_0^i-\mu_R)^2 - \\ &\frac{1}{2\tau_{R0}^{-2}}(\mu_R-\mu_{R0})^2 - (\mu_{R0}+1)\,ln\,\sigma_R^2 - \frac{\beta_{R0}}{\sigma_R^2} + C \end{aligned} \tag{25}$$

where C is a constant term independent of the parameters. According to Eq. (25), the derivation of μ_R:

$$\frac{\partial\, ln\, P}{\partial \mu_R} = \frac{1}{\sigma_R^2}\sum_{i=1}^{m}\left(R_0^i-\mu_R\right) - \frac{1}{\tau_{R0}^2}(\mu_R-\mu_{R0}) = 0 \tag{26}$$

The maximum a posteriori estimation value of μ_R:

$$\widehat{\mu_R} = \frac{\tau_{R0}^{-2}\mu_{R0}+m\sigma_R^{-2}\overline{R_0}}{\tau_{R0}^{-2}+m\sigma_R^{-2}} \tag{27}$$

Such that $x = \sigma_R^2$, the derivation of Eq. (25) gives:

$$\begin{aligned} \frac{\partial\, ln\, P}{\partial x} &= -\frac{m}{2x} + \frac{1}{2x^2}\sum_{i=1}^{m}\left(R_0^i-\mu_R\right)^2 - \\ &\frac{\alpha_{R0}+1}{x} + \frac{\beta_{R0}}{x^2} = 0 \end{aligned} \tag{28}$$

The maximum a posteriori estimation value of σ_R^2:

$$\widehat{\sigma_R^2} = \frac{2\beta_{R0}+\sum_{i=1}^{m}\left(R_0^i-\widehat{\mu_R}\right)^2}{2\alpha_{R0}+m+2} \tag{29}$$

Similarly, the MAP estimates of mean μ_S and variance σ_S^2 were calculated as shown in **Table 1.**

Table 1. The maximum a posteriori estimates of each parameter.

parameters	prior distribution	Posterior distribution	MAP estimate
μ_R	$N(\mu_{R0}, \tau_{R0}^2)$	$N(\widehat{\mu_R}, \widehat{\sigma_{\mu_R}^2})$	$\widehat{\mu_R} = \frac{\tau_{R0}^{-2}\mu_{R0}+m\sigma_R^{-2}\overline{R_0}}{\tau_{R0}^{-2}+m\sigma_R^{-2}}$
σ_R^2	$IGa(\alpha_{R0}, \beta_{R0})$	$IGa(\widehat{\alpha_R}, \widehat{\beta_R})$	$\widehat{\sigma_R^2} = \frac{2\beta_{R0}+\sum_{i=1}^{m}\left(R_0^i-\widehat{\mu_R}\right)^2}{2\alpha_{R0}+m+2}$
μ_S	$N(\mu_{S0}, \tau_{S0}^2)$	$N(\widehat{\mu_S}, \widehat{\sigma_{\mu_S}^2})$	$\widehat{\mu_S} = \frac{\tau_{S0}^{-2}\mu_{S0}+n\sigma_S^{-2}\overline{S}}{\tau_{S0}^{-2}+n\sigma_S^{-2}}$
σ_S^2	$IGa(\alpha_{S0}, \beta_{S0})$	$IGa(\widehat{\alpha_S}, \widehat{\beta_S})$	$\widehat{\sigma_S^2} = \frac{2\beta_{S0}+\sum_{j=1}^{n}\left(S_j-\widehat{\mu_S}\right)^2}{2\alpha_{S0}+n+2}$

4. Model-solving method based on the MCMC approach

The high number of parameters in Bayesian inference requires solving a high-dimensional integration problem in the posterior distribution to obtain the posterior distribution or posterior expectation. There is a nonlinear degeneracy relationship in $R(n) = R_0 - \sum_{i=1}^{n} k\,(S_i/S_e)^m$, which is difficult to be solved directly by traditional analytical methods. To overcome this problem, the Markov chain Monte Carlo (MCMC) method is used to solve the posterior distribution by sampling the parameters in simulation.

4.1. Model solution via Gibbs sampling in MCMC

The parameter vector $\theta = \{\mu_R, \sigma_R^2, \mu_S, \sigma_S^2\}$, whose joint posterior distribution can be expressed as:

$$p(\theta|D) \propto p(D|\theta) \cdot p(\mu_R) \cdot p(\sigma_R^2) \cdot p(\mu_S) \cdot p(\sigma_S^2) \tag{30}$$

where $p(D|\theta)$ is

$$p(D|\theta) = \left[\prod_{i=1}^{m} \frac{1}{\sqrt{2\pi\sigma_R^2}} exp(-\frac{\left(R_0^i-\mu_R\right)^2}{2\sigma_R^2})\right]\left[\prod_{j=1}^{n} \frac{1}{\sqrt{2\pi\sigma_S^2}} exp(-\frac{\left(S_j-\mu_S\right)^2}{2\sigma_S^2})\right] \tag{31}$$

where D is the observation data set, which contains the initial strength samples $\{R_0^1, R_0^2, \cdots, R_0^m\}$ and the working load samples $\{S_1, S_2, \cdots, S_n\}$;

Gibbs sampling, as the typical implementation of MCMC, constructs Markov chains by alternately sampling the conditional posterior distributions of each parameter. For the new equipment reliability model, the conditional posterior distribution of each parameter is derived as follows:

For the given $\sigma_R^2, \mu_S, \sigma_S^2$the conditional posterior of μ_R is:

$$p(\mu_R|\sigma_R^2, D) \propto p(D_R|\mu_R, \sigma_R^2) \cdot p(\mu_R) \tag{32}$$

Substituting the normal likelihood with the normal prior gives:

$$p(\mu_R|\sigma_R^2, D) \propto exp\left(-\frac{1}{2\sigma_R^2}\sum_{i=1}^{m}\left(R_0^i - \mu_R\right)^2\right) \cdot exp\left(-\frac{1}{2\tau_{R_0}^2}\sum_{i=1}^{m}\left(\mu_R - \mu_{R_0}\right)^2\right) \tag{33}$$

Eq. (33) combined, the conditional posterior of μ_R remains normally distributed:

$$\mu_R|\sigma_R^2, D \sim N\left(\frac{\frac{m}{\sigma_R^2}\overline{R_0}+\frac{1}{\tau_{R_0}^2}\mu_{R_0}}{\frac{m}{\sigma_R^2}+\frac{1}{\tau_{R_0}^2}}, \frac{1}{\frac{m}{\sigma_R^2}+\frac{1}{\tau_{R_0}^2}}\right) \tag{34}$$

Let $\lambda_R = \frac{m}{\sigma_R^2} + \frac{1}{\tau_{R_0}^2}$, the mean and variance are respectively:

$$E(\mu_R|\sigma_R^2, D) = \frac{\lambda_R^{-1}}{\sigma_R^2} m\overline{R_0} + \lambda_R^{-1}\tau_{R_0}^{-2}\mu_{R0} \tag{35}$$

$$Var(\mu_R|\sigma_R^2, D) = \lambda_R^{-1}\left(\frac{m}{\sigma_R^2}\overline{R_0} + \frac{1}{\tau_{R_0}^2}\mu_{R0}\right) \tag{36}$$

For the given μ_R, μ_S, σ_S^2 the conditional posterior of σ_R^2 is:

$$p(\sigma_R^2|\mu_R, D) \propto p(D_R|\mu_R, \sigma_R^2) \cdot p(\sigma_R^2) \tag{37}$$

Substitution of normal likelihood with inverse gamma prior:

$$p(\sigma_R^2|\mu_R, D) \propto (\sigma_R^2)^{-\frac{m}{2}} exp\left(-\frac{1}{2\sigma_R^2}\sum_{i=1}^{m}\left(R_0^i - \mu_R\right)^2\right) \cdot (\sigma_R^2)^{-\alpha_{R_0}-1} exp\left(-\frac{\beta_{R_0}}{\sigma_R^2}\right) \tag{38}$$

Integrating Eq. (38) gives:

$$p(\sigma_R^2|\mu_R, D) \propto (\sigma_R^2)^{-(\alpha_{R_0}+\frac{m}{2}+1)} exp\left\{-\frac{1}{\sigma_R^2}\left(\beta_{R_0} + \frac{1}{2}\sum_{i=1}^{m}\left(R_0^i - \mu_R\right)^2\right)\right\} \tag{39}$$

It can be seen that the conditional posterior of σ_R^2 is an inverse gamma distribution:

$$\sigma_R^2|\mu_R, D \sim IGa\left(\alpha_{R_0} + \frac{m}{2}, \beta_{R_0} + \frac{1}{2}\sum_{i=1}^{m}\left(R_0^i - \mu_R\right)^2\right) \tag{40}$$

The similar derivation can be obtained:

$$\mu_S|\sigma_S^2, D \sim N\left(\frac{\frac{n}{\sigma_S^2}\overline{S}+\frac{1}{\tau_{S_0}^2}\mu_{S_0}}{\frac{n}{\sigma_S^2}+\frac{1}{\tau_{S_0}^2}}, \frac{1}{\frac{n}{\sigma_S^2}+\frac{1}{\tau_{S_0}^2}}\right) \tag{41}$$

$$\sigma_S^2|\mu_S, D \sim IGa\left(\alpha_{S_0} + \frac{n}{2}, \beta_{S_0} + \frac{1}{2}\sum_{i=1}^{n}\left(S_j - \mu_S\right)^2\right) \tag{42}$$

4.2. Iterative process of Gibbs sampling for parameter update

In this paper, the MCMC method based on Gibbs sampling is employed to solve the posterior estimation problem. The mean of the prior distribution is chosen as the initial value, which avoids extreme initial values and improves the computational efficiency. Moreover, the prior distribution integrates simulated and historical data, so its mean can better represent the true parameter values than random initial values, reducing the "warm start" bias. Additionally, we have tried other solutions,

randomly generating initial values from the range of the prior distribution. If the value falls in a low-density area, it may lead to a slower convergence speed, which is not applicable to small sample cases.

The specific steps of Gibbs sampling are as follows:

Determine the initial value, set $\{\mu_R^{(0)}, \sigma_R^{2(0)}, \mu_S^{(0)}, \sigma_S^{2(0)}\}$, usually take the mean of the prior distribution, so that $\mu_R^{(0)} = \mu_{R_0}, \sigma_R^{2(0)} = \frac{\beta_{R_0}}{\alpha_{R_0}+1}$, and $\mu_S^{(0)}, \sigma_S^{2(0)}$ are initialized identically.

Set the number of iterations M. For $t = 1,2,\cdots,M$, update the components of the parameter vector in the following order.

Perform sampling iterations and update to the tth iteration.

Update $\mu_R^{(t)}$

Sample from conditional posterior distribution when the $\sigma_R^{2(t-1)}, \mu_S^{(t-1)}, \sigma_S^{2(t-1)}$ is known:

$$\mu_R^{(t)} \sim N\left(\frac{\tau_{R_0}^{-2}\mu_{R_0} + m\sigma_R^{-2(t-1)}\overline{R_0}}{\tau_{R_0}^{-2} + \sigma_R^{-2(t-1)}}, \frac{1}{\tau_{R_0}^{-2} + m\sigma_R^{-2(t-1)}}\right)$$

Update $\sigma_R^{2(t)}$

Sample from conditional posterior distribution when $\mu_R^{(t)}, \mu_S^{(t-1)}, \sigma_S^{2(t-1)}$ is known:

$$\sigma_R^{2(t)} \sim IGa\left(\alpha_{R_0} + \frac{m}{2}, \beta_{R_0} + \frac{1}{2}\sum_{i=1}^{m}\left(R_0^i - \mu_R^{(t)}\right)^2\right)$$

Update $\mu_S^{(t)}$

Sample from conditional posterior distribution when the $\mu_R^{(t)}, \sigma_R^{2(t)}, \sigma_S^{2(t-1)}$ is known:

$$\mu_S^{(t)} \sim N\left(\frac{\tau_{S_0}^{-2}\mu_{S_0} + n\sigma_S^{-2(t-1)}\overline{S}}{\tau_{S_0}^{-2} + n\sigma_S^{-2(t-1)}}, \frac{1}{\tau_{S_0}^{-2} + n\sigma_S^{-2(t-1)}}\right)$$

Update $\sigma_S^{2(t)}$

Sample from conditional posterior distribution when the $\mu_R^{(t)}, \sigma_R^{2(t)}, \mu_S^{(t)}$ is known:

$$\sigma_R^{2(t)} \sim IGa\left(\alpha_{S_0} + \frac{n}{2}, \beta_{S_0} + \frac{1}{2}\sum_{j=1}^{n}\left(S_j - \mu_S^{(t)}\right)^2\right)$$

Discard the results of M_0 iterations before the former Markov chain reaches a converged state and keep $\theta^{(t)} = \left(\mu_R^{(t)}, \sigma_R^{2(t)}, \mu_S^{(t)}, \sigma_S^{2(t)}\right)$;

The parameters to be estimated are computed and in this paper the sample mean is used as the parameter point estimate:

$$\widehat{\mu_R} = \frac{1}{M}\sum_{i=1}^{M}\mu_R^{(i)}$$

$$\widehat{\sigma_R^2} = \frac{1}{M}\sum_{i=1}^{M}\sigma_R^{2(i)} \tag{43}$$

The reliability a posteriori expectation is:

$$\hat{R}(n) = \frac{1}{M}\sum_{i=1}^{M}\int_{-\infty}^{+\infty}\left[1 - \Phi\left(\frac{r - k\sum_{j=1}^{n}\left(\frac{S_j}{S_e}\right)^m - \mu_S^{(i)}}{\sigma_S^{(i)}}\right)\right]\frac{1}{\sqrt{2\pi}\sigma_R^{(i)}}e^{\frac{\left(r-\mu_R^{(i)}\right)^2}{2\sigma_R^{2(i)}}}dr \tag{44}$$

It is simplified by the point estimation Eq (44):

$$\hat{R}(n) = \Phi\left(\frac{\overline{\mu_R} - n\cdot k\left(\frac{\overline{\mu_S}}{S_e}\right)^m - \overline{\mu_S}}{\sqrt{\overline{\sigma_R^2} + \overline{\sigma_S^2}}}\right) \tag{45}$$

In this section, the hyperparameter solution is performed by the MCMC method, and then the posterior distribution function is constructed to provide accurate parameter support for the reliability assessment and remaining life prediction of new equipment.

5. Bayesian estimation of reliability parameters for equipment

5.1. Prior information analysis and distribution characterization

In traditional reliability analysis, the sample data are often used directly as a prior samples, and the prior distribution estimation is realized by statistical mean and variance. The sample data of the initial strength and load of the new equipment is essentially the observation information containing the parameters $\mu_{Ri}, \sigma_{Ri}^2, \mu_{Si}, \sigma_{Si}^2$, but not the prior distribution of the parameters $\mu_{Ri}, \sigma_{Ri}^2, \mu_{Si}, \sigma_{Si}^2$ itself.

In this paper, reliability tests were conducted on a specific type of equipment, and the test standards conformed to those stipulated in GJB 899A-2009 "Reliability Evaluation and Acceptance Tests", regarding the initial mean strength μ_R, strength variance σ_R^2, working load mean μ_S, and load variance σ_S^2 of components. The prior information set containing 30 groups of samples was constructed. The specific parameter samples are shown in Table 2 below:

Table 2. Samples of parameters formed by prior information.

$\mu_R(MPa)$	$\sigma_R^2(MPa^2)$	$\mu_S(kN)$	$\sigma_S^2(KN^2)$
285.6347	18.3726	12.5418	3.95627
287.7264	12.5839	12.8725	2.87365
282.5836	21.4567	13.1258	3.56728
289.2583	15.6728	12.9854	3.12567
286.8742	10.2583	12.6758	2.58365
283.5632	19.8745	13.3258	3.75826
288.2587	13.5672	12.8452	2.75836
284.8362	17.5839	12.7258	2.65873
281.2583	18.7456	13.2583	3.65827
289.5836	14.5672	13.0258	3.25876
287.7421	11.2583	12.8754	2.85673
282.8365	20.5678	13.3582	3.85627
288.5832	16.5873	12.9583	3.15678
285.7632	12.8736	12.7854	2.75638
283.2586	19.5672	13.2853	3.75628
287.5832	13.8765	12.8521	2.85672
284.2583	17.5638	12.6758	2.65873
281.5836	18.7654	13.3258	3.85627
289.8365	14.5873	13.0583	3.25876
286.5632	11.5873	12.8254	2.85637
282.5638	21.5678	13.4258	3.95627
288.2587	16.5832	12.9853	3.15876
285.7362	12.5873	12.6758	2.75638
283.5836	19.5873	13.2586	3.75682
287.2583	13.5876	12.8521	2.85672
284.8365	17.5682	12.7258	2.65873
281.8362	18.5673	13.3582	3.85627
289.5638	14.5832	13.0258	3.25876
286.7421	11.5832	12.8754	2.85673
282.5836	20.5873	13.4582	3.95627

In Table 2, μ_{Ri} denotes the mean value of the initial strength of the equipment in the ith sample group,σ_{Ri}^2denotes the variance of the initial strength of the munition in the ith sample group, μ_{Si} denotes the mean value of the load in the ith sample group, and σ_{Si}^2 denotes the variance of the load in the ith sample group.

These parameters are quantitative descriptions of the initial strength and firing load distribution characteristics of the ammunitions under different impact load conditions, reflecting the concentration trend and degree of dispersion of the initial strength and firing load in the sample data.

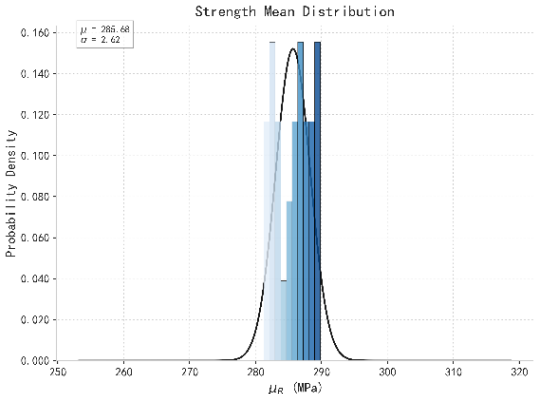

(a) μ_R histogram of frequency distribution

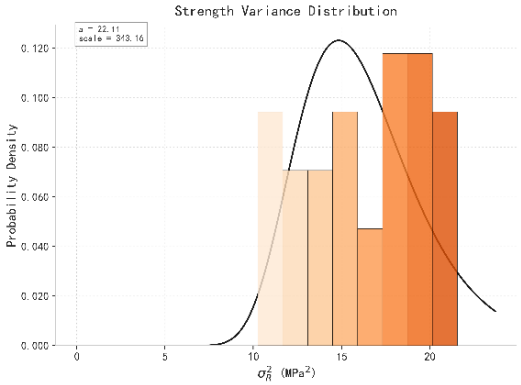

(b) σ_R^2 histogram of frequency distribution

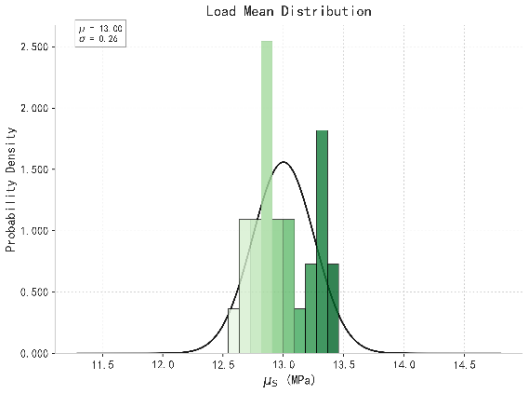

(c) μ_S histogram of frequency distribution

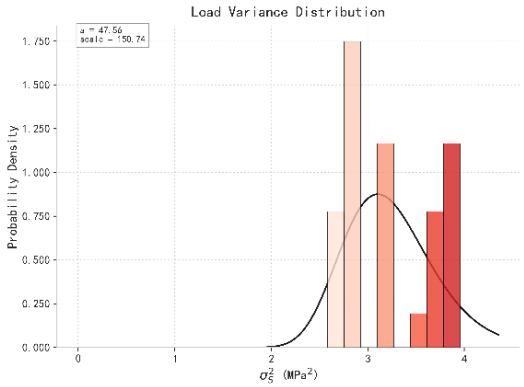

(d) σ_S^2 histogram of frequency distribution

Fig.1. Histogram of frequency distribution.

The histogram of the frequency density distribution plotted from the sample of Table 2 is shown in Fig.1, and the parameters μ_R and μ_S approximately follow the normal distribution, and $\boldsymbol{\sigma_R^2}$ and $\boldsymbol{\sigma_S^2}$ approximately follow the inverse gamma distribution. This is largely consistent with the pre-set assumptions, and the differences do not affect the rationality of the distribution assumption. This is because the prior sample size is only 30 groups, resulting in local fluctuations in the histogram; and the histogram represents the frequency distribution of discrete samples, while the inverse gamma distribution is the continuous distribution. The selection of the grouping interval will lead to deviations between the local frequency and the probability density.

The mean and variance of the four parameters are shown in Table 3:

Table 3. Mean and variance of parameters.

statistic	μ_R	σ_R^2	μ_S	σ_S^2
mean	285.6849	16.2240	13.0008	3.2380
variance	7.1135	11.2835	0.0678	0.2346

5.2. Determination of prior distribution hyperparameters

Based on the sample of a prior parameters of the initial strength and working load of the certain type of equipment, provided in Table 2,and the corresponding parameter means and variances in Table 3, the prior distribution hyperparameters are derived in conjunction with the theory of maximum the posteriori estimation.

Due to the small sample size, the rigorous statistical test of the goodness-of-fit of the selected the prior distributions is essential. Therefore, the K-S test was used for nonparametric validation of the distributional hypotheses.

The K-S test directly quantifies the maximum absolute deviation between the empirical cumulative distribution function (ECDF) and the hypothesized theoretical cumulative distribution function (CDF), and is particularly suitable for verifying the goodness-of-fit of the normal and inverse gamma distributions. The K-S test statistic is computed as:

$$D_n = sup_x |F_n(x) - F(x)| \tag{46}$$

where n is the sample size, $x$is a random variable, said to take all x values of the upper bound, $F_n(x)$ for the hypothesis distribution of the cumulative distribution function, $F(x)$ for the theoretical distribution of the cumulative distribution function to be tested.

Table 4. Hyperparameters in a prior distribution.

parameter	m	$IGa(\alpha,\beta)$				$N(\mu_0,\sigma^2/\kappa_0)$					
		$\hat{\alpha}$	$\hat{\beta}$	K-S test		$\hat{\mu}_0$	$\hat{\sigma}^2$	$(\sigma^2/\kappa_0)'$	κ_0	K-Stest	
				statistic	p					statistic	p
$P(\mu_R,\sigma_R^2)$	30	26.1321	407.7431	0.618	0.897	285.6849	7.1175	17.1135	0.417	0.1179	0.7547
$P(\mu_s,\sigma_s^2)$	30	48.2320	152.9370	0.497	0.214	13.0008	0.0678	10.0678	7.175	0.1516	0.4513

Based on the above Eq. (16)-(19) and the data in Tables 2 and 3, the hyperparameters corresponding to the prior distribution of the key parameters of this type of equipment are solved. As shown in Table 4, the test values p are all greater than 0.05, further verifying that the previously hypothesized prior distributions are valid.

The Bayesian estimation method is used to estimate the parameters of the initial strength R_0 of the equipment as well as the working load S_i, and the normal distribution is selected as the mean parameter μ_R, μ_S as the prior distribution, the inverse gamma distribution as the variance parameter σ_R^2, σ_S^2 prior distribution, combined with the MCMC sampling to obtain the characteristics of the posterior distribution, to obtain the initial strength R_0 and the working load S_i The distribution is shown in Fig.2:

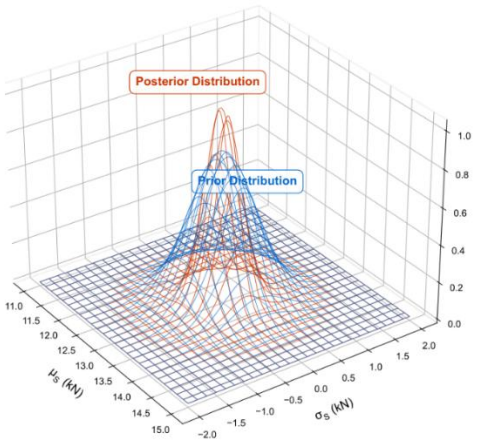

(a) Distribution of the initial strength parameter R_0 for equipment reliability

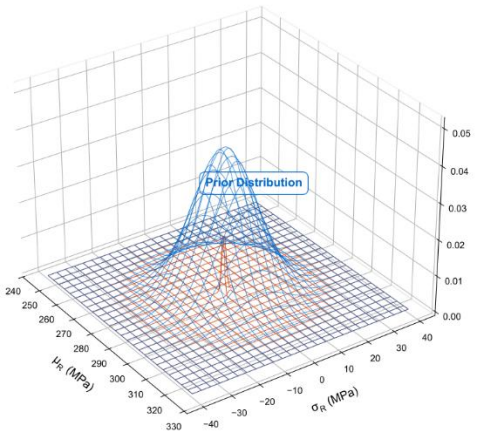

(b) Distribution of the initial strength parameter S_i for equipment reliability

Fig.2. Distribution of equipment reliability parameters.

The posterior distribution of the mean initial strength of the equipment in Fig. 2(a) shows a single-peaked normal pattern, with the mean of 285.97 MPa and 95% confidence interval of [283.86, 288.11] MPa; and the posterior distribution of the mean operating load is shown in Fig. 2(b), with a mean value of 12.955 kN and 95% confidence interval of [12.94, 12.98] kN.

After fusing the prior information with the experimental data, the fusion of the prior distribution and the likelihood function significantly improves the accuracy of parameter estimation, makes the posterior distribution more concentrated than the prior distribution, and effectively reduces the uncertainty of parameter estimation.

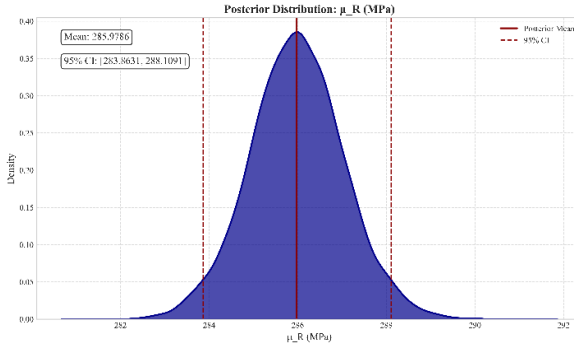

(a) The posterior distribution ofμ_R

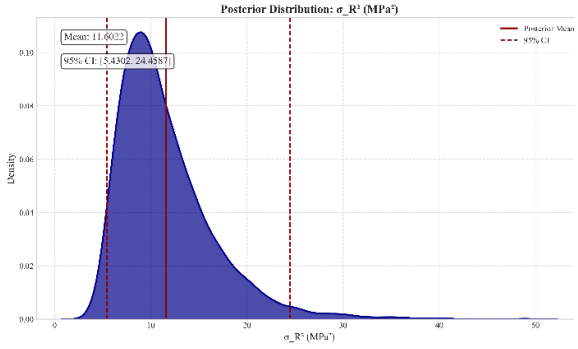

(b) The posterior distribution ofσ_R^2

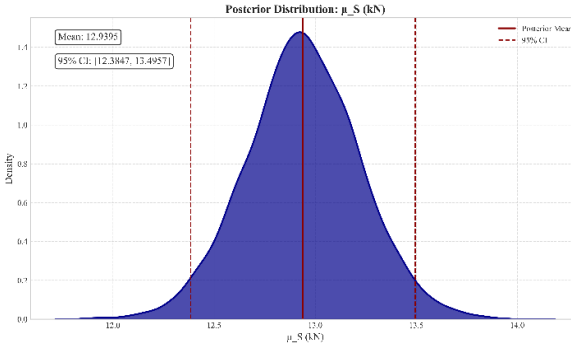

(c) The posterior distribution ofμ_S

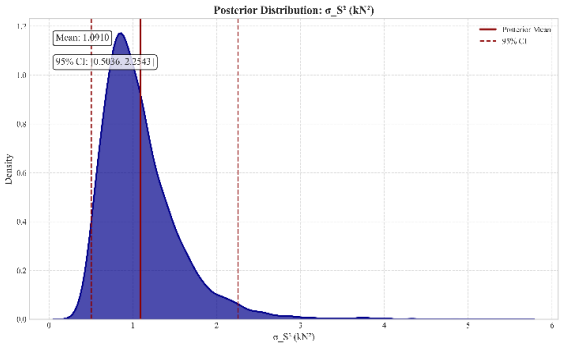

(d) The posterior distribution ofσ_S^2

Fig.3. Posterior distribution of hyperparameters.

In order to more closely visualize the posterior distribution of the parameters, the statistical characteristics of the key parameters are portrayed from the probability density dimension. In Fig. 3(a), the posterior distributions all show single peaks, the peaks of the curves correspond to the maximum the posteriori estimates of the parameters, and the means and 95% confidence intervals of the distributions accurately quantify the centralized trend of the parameter estimates.

Taking μ_R as an example, the median of its mean is close, indicating a good symmetry of the distribution, and the range of the 95% confidence interval intuitively reflects the confidence level of the theory on the inference of the initial intensity mean, the narrower the interval, the higher the estimation accuracy. The narrower the interval, the higher the estimation accuracy.$\mu_S$is similarly obtained, as shown in Fig.3 (b).

The posterior distribution of σ_R focuses on the discrete characteristics of the initial intensity, and its probability density also fits the inverse gamma curve to a high degree. As shown in Fig. 3 (c), the decay law and distribution pattern reveal the statistical distribution characteristics of the initial strength variance. The large dispersion of the distribution indicates that the intensity variance between equipment batches is significant. The μ_R is obtained as shown in Fig. 3 (d).

Based on the statistical logic analysis of Fig. 4, after first performing data preprocessing and setting the parameters of the prior distribution, the fit of the prior distribution and the sample data was verified by the KS test to ensure the reasonableness of the Bayesian inference. If the a priori test is

passed, the Gibbs sampling algorithm is used to perform MCMC iterations to derive the posterior distribution of the initial strength and load parameters;

Next, the time-varying reliability$R(t)$ is calculated over the whole life cycle of the equipment, and the mean, variance and confidence interval of the reliability are quantified by the statistical method of moments to fully characterize the uncertainty of the results.

Finally, the MCMC sampling convergence is checked (green cumulative mean curve adhering to the red overall mean line) to confirm the stability of parameter estimation; and the computed values of reliability are compared with the experimental test values to verify the model applicability. If the test is passed, the parameters are output; if the validation is not passed, the lower a priori distribution assumptions or MCMC sampling parameters are adjusted and the iterative process is re-executed.

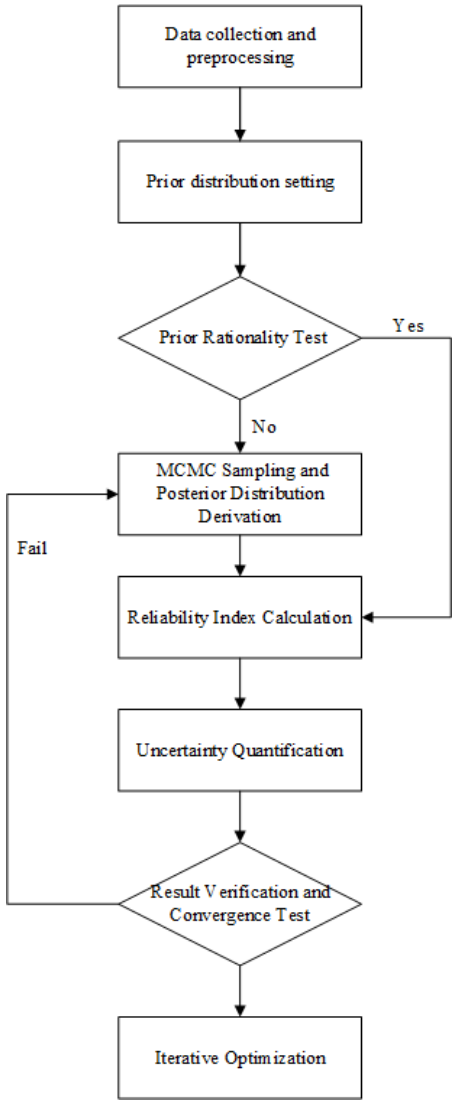

Fig.4. Convergence Verification Plots of Cumulative Means for MCMC Sampling Parameters.

5.3. Prior Sensitivity Analysis

To evaluate the robustness of the proposed Bayesian model with respect to the choice of prior distributions, the sensitivity analysis was conducted by varying the hyperparameters of the conjugate priors for the initial strength meanμ_R and working load meanμ_s.Three alternative prior settings were constructed:

(1) a conservative prior with mean shifted by -2σ σcalculated from baseline prior variance in Section 5.2) and variance increased by 50%;

(2) an optimistic prior with mean shifted by $+2\sigma$ and variance reduced by 50%;

(3) the non-informative prior approximated by setting the prior sample size to 1 (i.e., weakly informative normal-inverse-gamma priors).

For each prior setting, the posterior distributions of $\mu_R, \sigma_R^2, \mu_S, \sigma_S^2$were re-estimated using the same MCMC–Gibbs sampling scheme (5000 iterations, 1000 burn-in). The resulting posterior means and 95% credible intervals are summarized in Table 5. The RUL was defined as the number of working cycles when equipment reliability decreases to 0.5, which aligns with the RUL characterization standard to ensure consistency with the baseline model's performance evaluation.

Table 4. Posterior Estimates of Key Parameters and RUL Predictions Under Different Prior Settings

Prior Setting	$\hat{\mu}_R(MPa)$	$\hat{\mu}_S(kN)$	Predicted RUL
Original (Baseline)	285.97	12.955	153
Conservative Prior	284.12	12.892	152
Optimistic Prior	287.35	13.018	154
Weakly Informative Prior	285.61	12.947	153

The results show that despite substantial differences in prior assumptions, the posterior estimates of all key parameters remain highly consistent, with relative deviations in μ_R and $\mu_s$less than 0.8%. More importantly, the predicted RUL varies by no more than 2 cycles across all scenarios (152–154 cycles), which is well within the engineering tolerance for maintenance scheduling. This demonstrates that the proposed model is robust to reasonable variations in prior specification, and the integration of even moderately informative prior knowledge significantly stabilizes inference under small-sample conditions.

6. Experimental validation and comparison

To ensure the validity and reproducibility of the experimental data, the reliability tests in this study utilized calibrated and industry-recognized testing equipment. The specific specifications and functions of the key equipment are as follows: MTS 810 servo-hydraulic fatigue testing machine - This equipment is the core device used to apply cyclic dynamic loads to critical components. The equipment has passed national metrological certification within the past year, ensuring the reliability of the experimental data used for model validation. To assess the reliability of the key components of this equipment under high-stress conditions, 10 sets of sample data were obtained through accelerated life testing, as shown in Table 6. During the experiment, the strength and workload parameters of the equipment were monitored simultaneously. The initial strength was determined by the mechanical properties of the material test, while the working state was

collected in real time by dynamic sensors.

Table 6. Sample data collection for a new equipment type.

$\mu_R(MPa)$	$\sigma_R^2(MPa^2)$	$\mu_S(kN)$	$\sigma_S^2(KN^2)$
285.40216	17.34586	12.90677	3.08206
287.16282	14.87246	13.04457	3.05716
284.34492	18.03136	12.79237	3.63166
287.72072	14.49726	12.97127	3.19536
286.06282	16.04176	12.88257	2.94406
284.17622	18.72316	13.13497	3.85166
286.54072	15.29386	12.85127	2.83296
284.95212	16.76836	12.81677	2.72276
286.12082	16.38416	13.01787	3.39106

In Bayesian inference, the convergence of MCMC sampling directly determines the accuracy of parameter estimation. In this paper, based on the parameter prior distributions of the initial strength and working load of the equipment, combined with the external test experimental data, the solution is carried out using Bayesian WinBUGS software. Through MCMC combined with Gibbs sampling, the parameters $\mu_R, \sigma_R^2, \mu_S, \sigma_S^2$ are iteratively sampled from conditional probability.

The number of iterations is set to 5000, and the iterative trace map is generated, as shown in Fig.5. Where the iterative trace plots of $\mu_R, \sigma_R^2, \mu_S, \sigma_S^2$ correspond to Fig.5 (a)-(d), respectively:

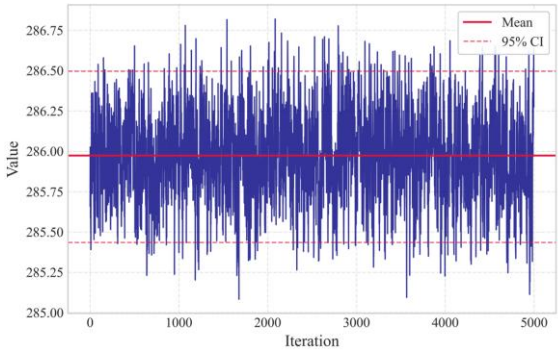

(a) The iterative tracking graph of the μ_R parameters

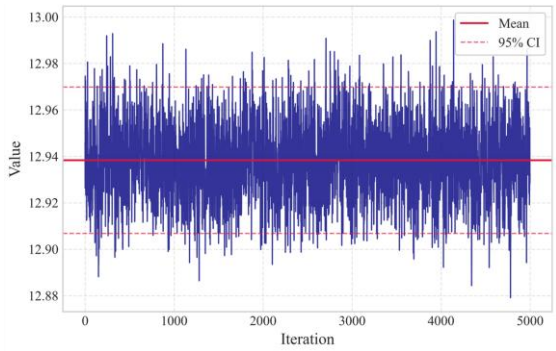

(b) The iterative tracking graph of the σ_R^2 parameters

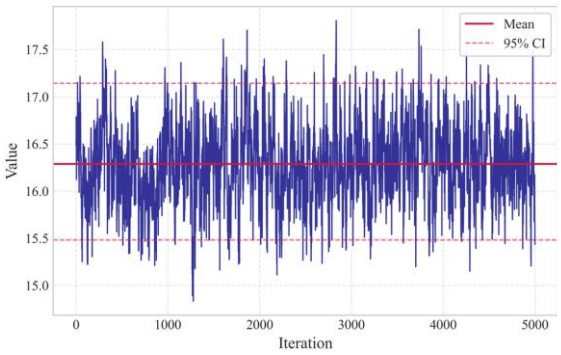

(c) The iterative tracking graph of the μ_S parameters

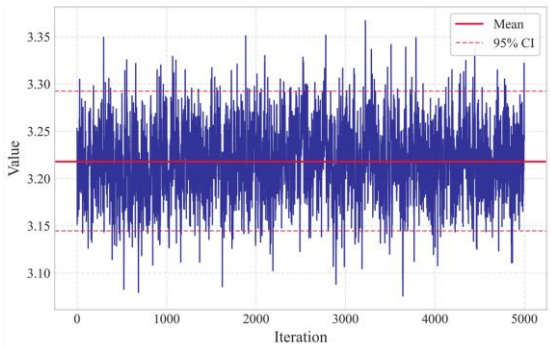

(d) The iterative tracking graph of the σ_S^2 parameters

Fig. 5. The iterative tracking graph of the $\mu_R, \sigma_R^2, \mu_S, \sigma_S^2$ parameters

For the initial strength mean value μ_R, as shown in Fig.5 (a), due to the chain's "hot start" effect in the initial iteration, the parameter mean value exhibits small fluctuations. However, after more than 2000 iterations, the mean value gradually converges and stabilizes at 285.98 MPa, with a fluctuation of less than 0.1%, indicating that the Markov chain has reached a stationary state.

Analyzing the trace plots of $\sigma_R^2, \mu_S, \sigma_S^2$ in Fig.5 (b)-(d), the parameter chains also show a similar pattern: multiple chains fluctuate synchronously around the overall mean during the iterative process, with no persistent drift or dispersion. This verifies the consistency and stability of the sampling process.

To further verify the independence of the Monte Carlo Markov chain samples, the autocorrelation graphs of the key parameters were plotted, as shown in Fig.6. The x-axis represents the lag order, and the y-axis represents the autocorrelation coefficient:

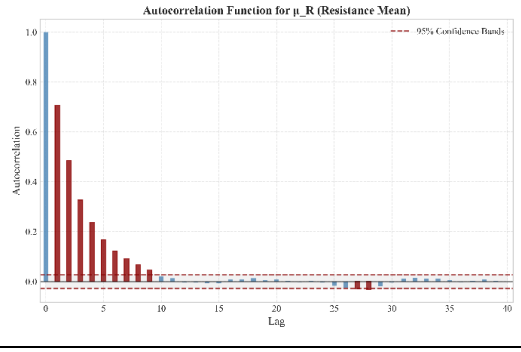

(a) Autocorrelation graph of μ_R

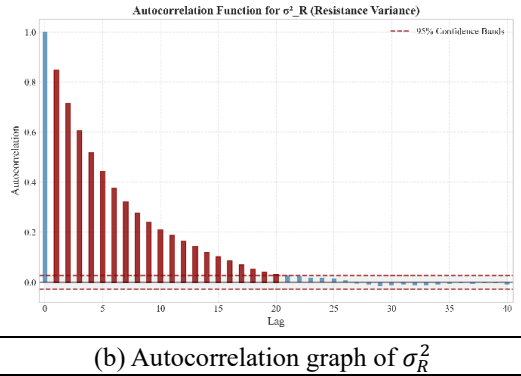

(b) Autocorrelation graph of σ_R^2

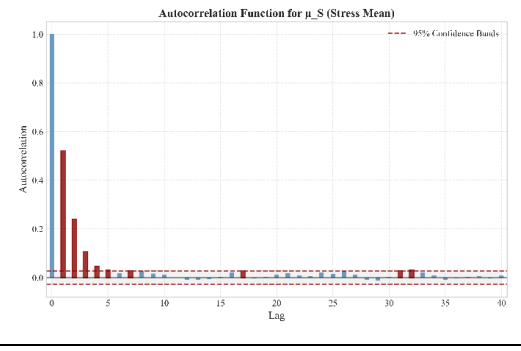

(c) Autocorrelation graph of μ_S

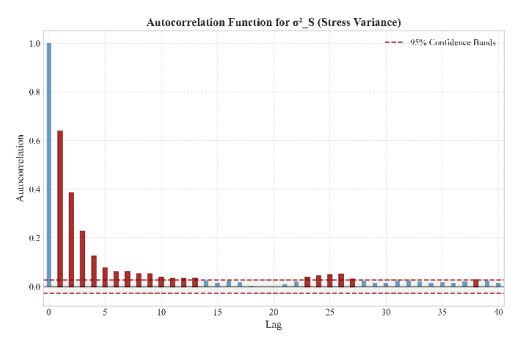

(d) Autocorrelation graph of σ_S^2

Fig.6. Autocorrelation graph of $\mu_R, \sigma_R^2, \mu_S, \sigma_S^2$

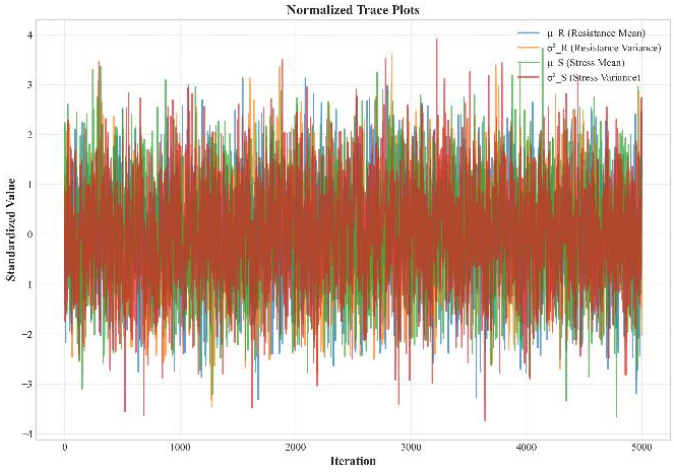

Fig.7. Multi-chain comparison trajectory diagram.

Fig.7 illustrates the iterative trajectories of the key parameters $\mu_R, \sigma_R^2, \mu_S, \sigma_S^2$ during the MCMC sampling process. The trajectories of all parameters do not show any persistent trends or drift after 5000 iterations, but instead fluctuate within a stable range. This indicates that the Markov chain has converged, thereby ensuring the reliability of the posterior inference in the small sample reliability analysis.

For $\mu_R, \sigma_R^2, \mu_S, \sigma_S^2$, when the lag order exceeds 20, the autocorrelation coefficient will drop below 0.1. This indicates that there is the relatively weak correlation between adjacent samples - this meets the "approximate independence" requirement of the MCMC sampling, thereby ensuring that the sampled values can effectively cover the posterior distribution.

Convergence from the cumulative mean to further verify the smoothness of MCMC sampling. The Running Mean plots corresponding to different parameters (cumulative mean on the vertical axis, number of iterations on the horizontal axis, and overall mean on the red dashed line) are shown in Fig.8.

When the number of iterations in the initial stage is less than 1000, the Markov chain is affected by the initial value, and the green curve (running mean) deviates significantly from the red dashed line (overall mean), with more drastic fluctuations.

Since the chain has not yet fully traversed the posterior distribution, the cumulative mean is disturbed by the starting sampling point. As the iteration progresses, the green curve gradually narrows and adheres to the red dashed line, and the fluctuation amplitude continues to decrease. As shown in Fig.8, the curve stabilizes at a certain mean value after 1000 iterations. This indicates that the cumulative mean gradually approaches the overall mean as the range of sampling covering the posterior distribution expands, verifying the smoothness of the MCMC chain and the unbiasedness of sampling.

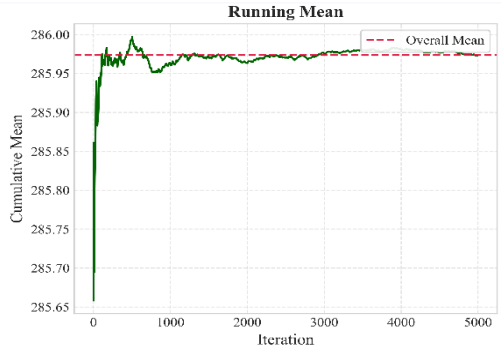

(a) The iterative tracking graph of strength mean μ_R

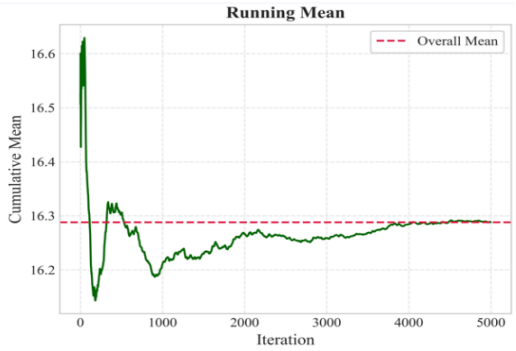

(b) The iterative tracking graph of strength mean σ_R^2

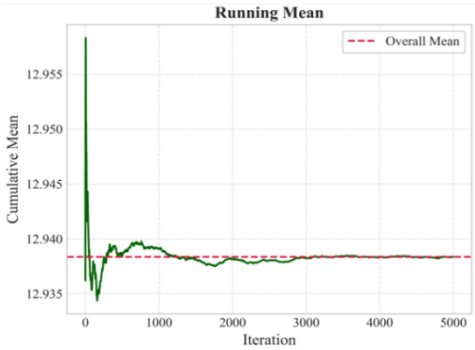

(c) The iterative tracking graph of strength mean μ_S

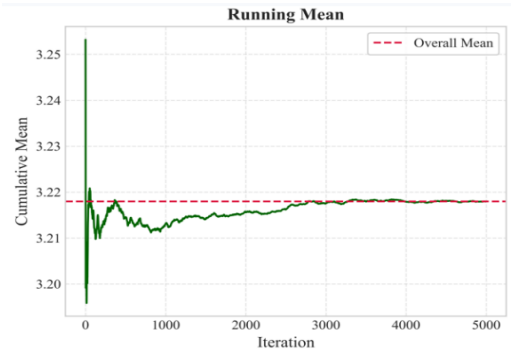

(d) The iterative tracking graph of strength mean σ_S^2

Fig.8. The iterative tracking graph of the $\mu_R, \sigma_R^2, \mu_S, \sigma_S^2$ parameters

Parameter kernel density maps were plotted, as shown in Fig.9, to enable a more intuitive understanding of the parameter distributions.

The newly developed equipment, whose initial strength R_0 obeys a normal distribution, is estimated by Bayesian posterior estimation with mean $\mu_{R_0} = 285.98MPa$ and the standard deviation $\sigma_{R_0} = 16.3MPa$. The working load S to which the equipment is subjected obeys a normal distribution, which is corrected statistically and with Bayesian correction, with the mean value of the load $\mu_S = 12.94\ kN$ and the standard deviation $\sigma_S = 3.22\ kN$.

The mean of the working load is stable and the coefficient of variation is low, so the time-varying degradation model can be constructed based on the mean value of the load and the fatigue life. Based on the theory of material fatigue damage accumulation, combined with the material test and simulation analysis of the key components of the new equipment, it is determined that the material fatigue characteristic constant m=2.5, k=28.5.

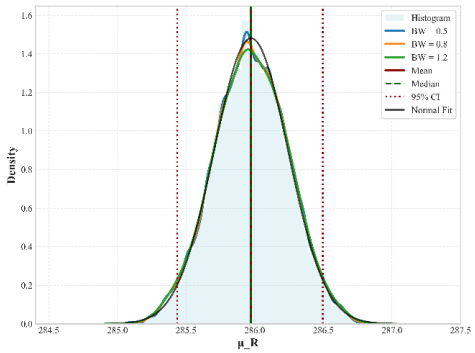

(a) Kernel density map of initial strength mean μ_R

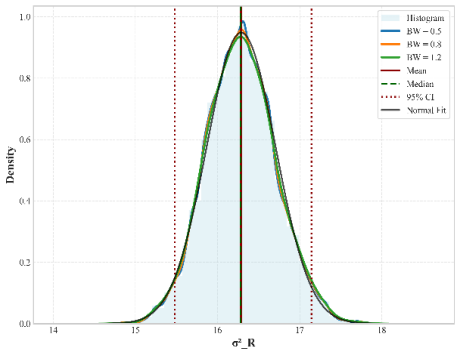

(b) Kernel density map of initial strength variance σ_R^2

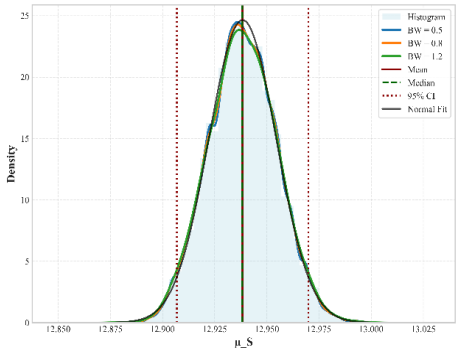

(c) Kernel density map of load mean μ_S

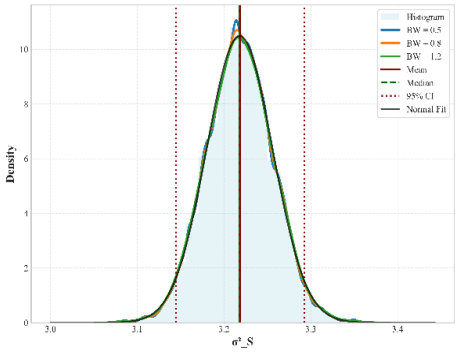

(d) Kernel density map of load variance σ_S^2

Fig.9, Kernel density map for parameter $\mu_R, \sigma_R^2, \mu_S, \sigma_S^2$

Based on the above degradation model, two types of time-varying reliability assessment models are constructed to carry out comparative studies. The reliability degradation comparison curves are plotted with the number of cyclic loads n as the horizontal coordinate and the equipment reliability $R(n)$ as the vertical coordinate. According to the relevant design specifications, determine the material fatigue characteristic constant $k = 28.5$, calculated new equipment reliability $R(t)$ and probability density $f(t)$ with the number of times of use changes in the law, respectively, as shown in Fig.10 (a) (b).

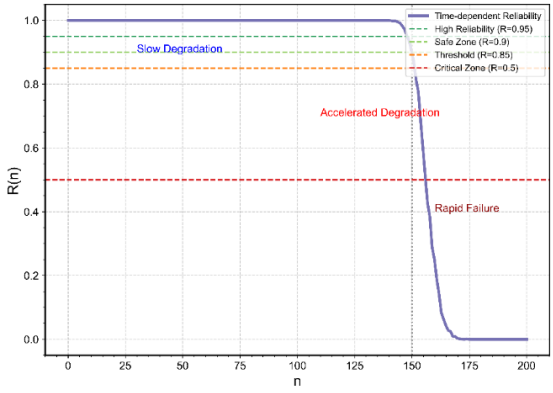

(a) Reliability of new equipment $\boldsymbol{R(t)}$

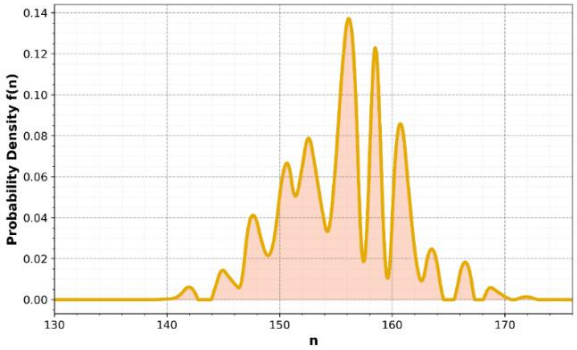

(b) Probability density of new equipment $f(t)$

Fig.10. Time-varying reliability assessment of new equipment

Fig.10 (a) shows that in the early stage of the device (up to 140 uses), the reliability is close to 1, indicating that the probability of random failure is extremely low at this stage. Subsequently, the reliability decreases sharply indicating that the device enters a fatigue damage dominated wear-out period. And Fig.10 (b) has a very high probability of fluctuation within 145 to 165 times, indicating that increased fatigue damage occurs within this phase, which also contributes to the sharp decrease in reliability.

As shown in Fig.11, $R_1(t)$ is a time-varying reliability model incorporating Bayesian small-sample information, which makes full use of the prior knowledge and experimental data to correct the parameter uncertainty; $R_2(t)$ is the traditional empirical model, relying on large sample assumptions and fixed parameter modeling. From the degradation trend, the reliability of the predictive models of both models degraded exponentially with the increase of the number of cycles n, which is highly compatible with the cumulative fatigue damage law of the material.

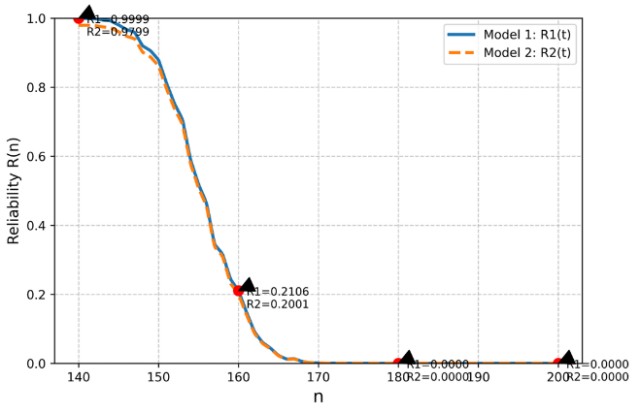

Fig.11. Comparative analysis of the results

To make the comparison results clearer and more intuitive, 135-159 times were selected as the core comparison interval, as shown in Table 6. In the stable stage of equipment performance, due to the small fluctuation of load distribution and initial strength characteristics, the predicted results of the two models are highly overlapped (when n=140,$R_1 \approx 0.9999$, $R_2 \approx 0.9909$), verifying the applicability of the traditional model under ideal working conditions. After the number of uses increases to 150, the device enters an accelerated degradation phase, and $R_1(t)$ is corrected to the posterior distribution through a Bayesian updating mechanism, which is more sensitive to the trend of reliability decay (when n=150,$R_1 \approx 0.8679, R_2 \approx 0.8506$). As the number of uses` continues to increase to the point where the device tends to

approach the failure critical state, $R_1(t)$ has a higher accuracy in identifying the failure critical point.

Table 7. Sample data collection for the new equipment type.

t	$R_1(t)$	$R_2(t)$	$\delta(\%)$
135	1.000 000	0.970 300	2.970 000
136	0.999 999	0.979 999	2.000 000
137	0.999 880	0.979 885	2.001 500
138	0.999 876	0.979 778	2.010 002
139	0.999 768	0.979 670	2.010 501
140	0.999 500	0.979 505	2.000 500
141	0.999 082	0.979 290	1.981 001
142	0.994 869	0.975 180	1.979 002
143	0.991 972	0.972 275	1.985 003
144	0.995 532	0.975 830	1.979 001
145	0.986 327	0.966 725	1.987 002
146	0.974 888	0.955 495	1.989 003
147	0.964 599	0.945 100	1.990 001
148	0.926 788	0.908 285	1.996 002
149	0.899 240	0.881 340	2.001 001
150	0.867 960	0.850 700	1.988 002
151	0.805 548	0.789 650	1.973 001
152	0.750 564	0.735 680	1.983 002
153	0.676 048	0.662 150	2.055 003
154	0.622 895	0.610 750	1.949 001
155	0.579 976	0.568 450	1.987 002
156	0.474 092	0.464 700	1.981 001
157	0.357 153	0.350 100	1.975 002
158	0.322 671	0.316 300	1.975 001
159	0.218 203	0.213 900	1.972 002

The comparison results are more clear and intuitive, 135-159 times were selected as the core comparison interval, as shown in Table 7.

To quantify the prediction accuracy of different models, the three-dimensional error analysis surface is constructed with the number of uses n, the material fatigue property constant k as the independent variables, and the relative reliability error $\delta(\%)$as the dependent variable, as shown in Fig. 12.

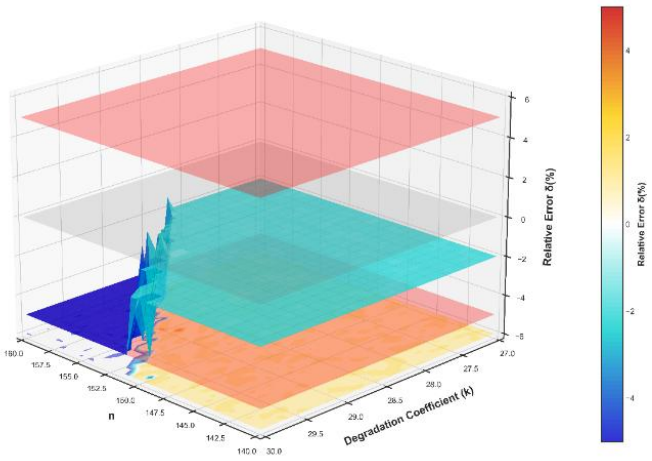

Fig. 12. Error analysis surfaces.

Although the prediction index $R_2(t)$ of the traditional empirical model is not the actual value but an estimated one, it is reasonable to use it as a comparison benchmark in this case. The reason is that this is both in line with academic standards and engineering practice: traditional models have been widely used and highly recognized in small sample reliability assessment for a long time 20, and their results are often used to evaluate the performance of new methods in industrial scenarios, thereby ensuring that the advantages of the model we propose are comparable.

The comparative analysis of the results of the two models shows that:

The two reliability change curves are in good agreement, with the relative error remaining within 2.0% across the region.

In the early stage of stable operation and the end of life of the equipment, the calculation errors of both models are small.

The degradation trend is “slow and then fast”.

In the interval of 135-159 times of use, the reliability calculated by the Bayesian time-varying reliability model based on small samples proposed in this paper is slightly higher than that of the traditional empirical model.

Based on Fig.s. 10, 11 and Table 7, it can be seen that the life cycle of the new equipment is divided into three stages and reliability is analyzed:

i) The early stage (1 - 140 cycles): The reliability is close to 1. The advantage of the Bayesian model lies in integrating prior information, correcting the over-conservatism of traditional models, and avoiding the underestimation of initial reliability due to the randomness of small samples.

ii) The middle stage (141 - 160 cycles): The Bayesian model shows superiority over the traditional model in terms of lag. This is because the Bayesian model integrates the fatigue parameters obtained from simulations, accurately capturing the initial situation of fatigue cracks.

iii) The late stage (>160 cycles): The reliability of the Bayesian model drops below 0.1, providing a 3 to 5 cycle early warning for equipment replacement, while the prediction of the traditional model lags by 5 to 8 cycles, which is crucial for avoiding sudden failures in engineering.

To further verify the superiority of the model proposed in this paper under the condition of small sample size, in addition to comparing with the finite element model, this section selects three typical basic methods mentioned in the introduction for parallel prediction results of each method are compared. The specific data are shown in Table 8.

Table 8. Comparison of Reliability Prediction Values.

t	Time-varying reliability model	Linear regression model Błąd! Nie można odnaleźć źródła odwołania.	Gray - Neural Network	Tribology Coupling model	FEA model
135	1.000 000	0.951 300	0.981 100	0.974 400	0.970 300
145	0.986 327	0.938 293	0.967 684	0.961 077	0.966 725
155	0.579 976	0.551 731	0.569 014	0.565 129	0.568 450
$\delta(\%)$	1.24%	4.87%	1.89%	2.56%	—

Based on the comparison of the reliability prediction values in Table 8, it can be concluded that the average relative error of the time-varying reliability model proposed in this paper is significantly better than that of the linear regression model, the tribology coupling model, and the grey-neural network model. In terms of accuracy, it demonstrates the significant advantage.

7. Conclusion

The Bayesian estimation method for equipment reliability with normal life is proposed, and the time-varying reliability assessment framework for the new type of equipment is constructed. The accurate prediction of reliability degradation over the whole life cycle of this equipment is realized by using the number of uses as the core life indicator. Compared with the existing reliability assessment studies, this study makes full use of the equipment reliability field test information and simulation test information, effectively integrates the prior information with the small-sample test data, and effectively solves the problem of insufficient precision of parameter estimation under the small-sample conditions of the traditional methods. And under the premise of ensuring the error accuracy, the reliability assessment of new equipment can be completed quickly.

In addition to the above advantages, this paper also has some limitations, for example, this paper requires that the prior information of the equipment has high reliability. If the prior information is not reliable, it will affect the estimation accuracy of equipment reliability. In addition, this paper only studies the reliability of equipment with normal-type life distributions, while the Weibull distribution, lognormal distribution and other distributions will be further explored in future studies.

References

1. Y. Z. Zhang, F. Han, and F. Yang, "Reliability analysis of small-sample failure data for random truncation high-voltage relay," *Appl. Sci.*, vol. 14, no. 11, p. 4950, 2024, doi: 10.3390/app14114950.
2. J. Hou, R. H. Wang, J. J. Wang, and Z. Yang, "Research on evaluation index system of information system equipment system contribution rate," *MATEC Web Conf.*, vol. 336, no. 11, pp. 28–43, 2021, doi: 10.1051/matecconf/202133605028.
3. Y. M. Yan, J. Y. Zhou, and Y. Yin, "Reliability estimation of retraction mechanism kinematic accuracy under small sample," *Eksploatacja i Niezawodnosc - Maintenance and Reliability*, no. 1, p. 174777, 2024, doi: 10.17531/ein/174777.
4. R. D. Zhao, X. M. Shi, Q. Wang, X. B. Su, and X. Song, "Bayesian inference for ammunition demand based on Gompertz distribution," *J. Syst. Eng. Electron.*, vol. 31, no. 3, pp. 567–577, 2020, doi: 10.23919/JSEE.2020.000035.
5. Q. Zhao, X. Jia, Z. J. Cheng, and B. Guo, "Bayesian estimation of residual life for Weibull-distributed components of on-orbit satellites based on multi-source information fusion," *Appl. Sci.*, vol. 9, no. 15, pp. 111–125, 2019, doi: 10.3390/app9153017.
6. A. Loganathan and M. Gunasekaran, "Construction of reliability single sampling plans based on exponentiated exponential distribution," *J. Test Eval.*, vol. 47, no. 2, pp. 594–607, 2018, doi: 10.1520/JTE20160594.
7. X. Y. Zhang, L. H. Yang, X. F. Han, Q. Zhang, C. P. Shi, and Z. Li, "A review of the mathematical evaluation model of contribution rate of weapon equipment system," *Acad. J. Comput. Inf. Sci.*, vol. 5, no. 6, pp. 97–111, 2022, doi: 10.25236/AJCIS.2022.050607.
8. M. Lu and Y. Xie, "Intelligent detection system for electrical equipment based on deep learning and infrared image processing technology," *Int. J. Adv. Comput. Sci. Appl.*, vol. 14, no. 8, pp. 1147–1155, 2023. https://doi.org/10.14569/IJACSA.2023.01408124
9. Q. Meng, J. Yang, and Y. Zhang, "A robot system for rapid and intelligent bridge damage inspection based on deep-learning algorithms," *J. Perform. Constr. Facil.*, vol. 37, no. 6, 2023, Art. no. 04023052, doi: 10.1061/JPCFEV.CFENG-4433.
10. Z. Xia, Y. Liu, and H. Ling, "Design of real-time monitoring and management system for digital power grid equipment based on intelligent

analysis," in *Proc. 2024 Int. Conf. Power, Electr. Eng., Electron. Control (PEEEC)*, 2024, pp. 562–567. https://doi.org/10.1109/PEEEC63877.2024.00108

11. D. Sun, "Research on abnormal detection and intelligent diagnosis algorithm of reservoir test data," in *Proc. 2024 Int. Conf. Power, Electr. Eng., Electron. Control (PEEEC)*, 2024, pp. 668–672. https://doi.org/10.1109/PEEEC63877.2024.00126
12. Y. Wang, "Research on accelerated degradation test and reliability evaluation method of electromechanical products," in *Proc. 33rd Chin. Control Decis. Conf.*, vol. 13, no. 2, 2021, pp. 260–265, doi: 10.1109/CCDC52312.2021.9601695.
13. K. Li, X. M. Shi, G. N. Li, and H. B. Liu, "Estimation method of anti-cruise missile hit probability based on normal-inverse gamma distribution," *Syst. Eng. Electron.*, vol. 44, no. 8, pp. 2621–2627, 2022, doi: 10.12305/j.issn.1001-506X.2022.08.27.
14. J. Madhumitha and G. Vijayalakshmi, "Bayesian reliability estimates of linear/circular consecutive k-out-of-n: F system based on Weibull distribution," *Int. J. Perform. Eng.*, vol. 16, no. 10, pp. 1509–1516, 2020, doi: 10.1063/5.0108545.
15. M. Compare, P. Baraldi, I. Bani, E. Zio, and D. McDonnell, "Industrial equipment reliability estimation: A Bayesian Weibull regression model with covariate selection," *Reliab. Eng. Syst. Saf.*, vol. 200, no. 2, pp. 65–80, 2020, doi: 10.1016/j.ress.2020.106891.
16. H. B. Liu and X. M. Shi, "Damage effectiveness calculation of hitting targets with ammunition based on Bayesian multinomial distribution," *Symmetry*, vol. 14, no. 5, pp. 71–84, 2022, doi: 10.3390/sym14050892.
17. J. R. Tanzer and L. L. Harlow, "Bayesian modeling of test reliability," *Multivar. Behav. Res.*, vol. 56, no. 1, pp. 159–179, 2020, https://doi.org/10.1080/00273171.2020.1854082
18. Z. Lv, J. Guo, and H. Lv, "Safety Poka Yoke in zero-defect manufacturing based on digital twins," *IEEE Trans. Ind. Informatics*, vol. 19, no. 2, pp. 1176–1184, 2023, doi: 10.1109/TII.2021.3139897.
19. B. Wang, P. Jiang, and B. Guo, "Reliability evaluation of aerospace valve based on multi-source information fusion," *Acta Armamentarii*, vol. 43, no. 1, pp. 199–206, 2022, doi: 10.3969/j.issn.1000-1093.2022.01.022.
20. D. F. Alex, Y. Nita, L. Trung, and Y. O. Prakash, "A deep neural network and Bayesian method based framework for all-terminal network reliability estimation considering degradation," *Reliab. Eng. Syst. Saf.*, vol. 229, no. 5, pp. 102–115, 2023, doi: 10.1016/j.ress.2022.108881.
21. K. M. Rastogi and P. E. Oguntunde, "Classical and Bayes estimation of reliability characteristics of the Kumaraswamy-Inverse Exponential distribution," *Int. J. Syst. Assurance Eng. Manag.*, vol. 10, no. 2, pp. 190–200, 2019, doi: 10.1007/s13198-018-0744-7.
22. R. Zahra, J. B. Ezzatallah, and D. Einolah, "Parameters and reliability estimation for the Weibull distribution based on intuitionistic fuzzy lifetime data," *Complex Intell. Syst.*, vol. 8, no. 6, pp. 481–496, 2022, doi: 10.1007/s40747-022-00720-x.
23. E. E. Nwezza and F. I. Ugwuowo, "An extended normal distribution for reliability data analysis," *J. Stat. Manag. Syst.*, vol. 25, no. 2, pp. 369–392, 2022, doi: 10.1080/09720510.2021.1878632.
24. L. L. Wu and G. Pan, "Expert information fusion method for reliability test evaluation of small sample complex products," *Mach. Electron.*, vol. 13, no. 11, pp. 3–6, 2014.
25. B. T. Chen, Y. Liu, C. H. Zhang, and Z. R. Wang, "Time series data for equipment reliability analysis with deep learning," IEEE Access, vol. 8, pp. 484–493, 2020, doi: 10.1109/ACCESS.2020.3000006.
26. Y. J. Guo, H. D. Wang, Y. Guo, M. J. Zhong, Q. Li, and C. Gao, "System operational reliability evaluation based on dynamic Bayesian network and XGBoost," Reliab. Eng. Syst. Saf., vol. 225, no. 6, pp. 178–193, 2022, doi: 10.1016/j.ress.2022.108622.
27. C. X. Jia, H. Y. Ding, and X. Zhang, "Reliability evaluation of direct current distribution system for intelligent buildings based on big data analysis," Tehnički Vjesnik, vol. 28, no. 5, pp. 121–135, 2021, doi: 10.17559/TV-20210507090202.
28. T. Chen, Z. Y. Liu, and L. Ju, "Improved Bayes-based reliability prediction of small-sample Hall current sensors," Machines, vol. 12, no. 9, p. 618, 2024, doi: 10.3390/machines12090618.
29. L. Dai, J. Y. Guo, and J. L. Wan, "A reliability evaluation model of rolling bearings based on WKN-BiGRU and Wiener process," Reliab. Eng. Syst. Saf., vol. 225, no. 9, pp. 55–68, 2022, doi: 10.1016/j.ress.2022.108646.